Curcumin-loaded polysaccharide nanoparticles: Optimization and anticariogenic activity against Streptococcus mutans

Article *in* Materials Science and Engineering C · March 2017

DOI: 10.1016/j.msec.2017.03.032

CITATIONS
4

READS
195

6 authors, including:

Amir Maghsoudi
Persisgen Par Co.
9 PUBLICATIONS **122** CITATIONS
SEE PROFILE

Saleheh Shahmoradi
University of Tehran
10 PUBLICATIONS **10** CITATIONS
SEE PROFILE

Ghassem Amoabediny
University of Tehran
80 PUBLICATIONS **321** CITATIONS
SEE PROFILE

Materials Science and Engineering C 75 (2017) 1259–1267

Contents lists available at ScienceDirect

Materials Science and Engineering C

journal homepage: www.elsevier.com/locate/msec

Curcumin-loaded polysaccharide nanoparticles: Optimization and anticariogenic activity against *Streptococcus mutans*

Amir Maghsoudi [a,*], Fatemeh Yazdian [b], Saleheh Shahmoradi [b], Leila Ghaderi [b], Mehran Hemati [c], Ghassem Amoabediny [d]

[a] Department of Industrial Biotechnology, National Institute of Genetic Engineering and Biotechnology, Tehran, PO Box 14965-161, Iran
[b] Department of Life Science Engineering, Faculty of New Science and Technologies, University of Tehran, Tehran, Iran
[c] Research and Entrepreneurship Center, Amirkabir University, Tehran, Iran
[d] Department of Chemical Engineering, Faculty of Engineering, University of Tehran, Tehran, Iran

ARTICLE INFO

Article history:
Received 7 October 2016
Received in revised form 25 February 2017
Accepted 3 March 2017
Available online 07 March 2017

Keywords:
Curcumin
Polysaccharide
Nanoparticle
Desolvation
Streptococcus mutans

ABSTRACT

Curcumin was loaded into different polysaccharide nanoparticles chitosan, alginate and starch, using the desolvation method. Curcumin-loaded nanoparticles exhibited enhanced solubility in aqueous solutions comparing with free curcumin. Effects of formulation parameters such as curcumin concentration and different volumes of ethanolic solution were affected the particle size and loading efficiency. Under optimum conditions, curcumin-loaded chitosan, starch and alginate nanoparticles with mean particles sizes of 66.3, 61.1 and 78.8 nm, and maximum loading efficiencies of 11.9%, 14.3% and 13.35% were achieved, respectively. Additionally, the minimum inhibitory concentration for chitosan, starch and alginate nanoparticles against the microorganism, *Streptococcus mutans*, were 0.114, 0.204 and 0.204 mg/mL, respectively. Curcumin was observed to release from nanoparticles under physiological pH over a period of 96 h. The effect of curcumin-loaded nanoparticles on *S. mutans* biofilms was assessed on dental models. According to the results, curcumin-loaded chitosan nanoparticles hold promises for being used in dental decay fighting products.

1. Introduction

The most common dental diseases in humans, are caries and periodontal illness, such as gingivitis and periodontitis. Many pharmaceutical dosage forms have been developed for the local therapy of dental problems and diseases affecting the oral cavity; dentifrices and mouth rinses as the most common. The short retention time in the oral cavity because of salivation, the intermittent swallowing, food and beverage intake as well as abrasion by soft tissue movements are the drawbacks of conventional systems [1].

Due to bacterial resistance to antibacterial agents such as antibiotics, development of new vanquisher antibacterial agents has become the subject of ongoing research [2]. So, development of dentifrices and mouthwashes, which their function is based on targeting these highly adaptable oral organisms and blocking their key mechanisms of phenotypic variation, are increasing. Using antimicrobial systems which diffuse across all biofilm structures is one way to achieve the goal. Nanoscale systems from natural polymers can be used as biological carriers within biofilms [3]. Some of advantages of polymeric nanoparticles are: increased stability of volatile pharmaceutical agents, easy and cheap fabrication in large quantities by a multitude of methods, significant improvement over traditional oral and intravenous methods of administration in terms of efficiency and effectiveness, delivering a higher concentration of pharmaceutical agent to a desired location, modifiable drug release, and easy incorporation into other activities related to drug delivery [4].

Streptococcus mutans is the main etiological agent in dental caries. Additionally, this bacterium is a major factor of infective endocarditis through carbohydrate fermentation of food into lactic acid fallowed by enamel demineralization. *S. mutans* presents extra surface proteins which many of them are toxic [5]. The first step for dental caries is the binding of bacteria to teeth surface. *S. mutans* creates sucrose related connections through glucosyltransferase and binding proteins to glucan and makes stable biofilms called dental plaque [6]. There are several approaches to prevent dental decay. One approach is the reduction of carbohydrate consumption with the aid of different types of sugar substitutes including artificial sweeteners such as saccharin and natural sweeteners like xylitol. Another alternative is to use dental sealants which are applied to protect tooth surfaces with deep grooves and pores. Fluoride consumption is another method that shows its anti-dental decay effects through substitution of hydroxyl groups in hydroxy apatite and formation of fluorapatite during the formation of enamel, improving the remineralization of initial caries lesions in enamel and

* Corresponding author.
E-mail address: maghsoudi@nigeb.ac.ir (A. Maghsoudi).

http://dx.doi.org/10.1016/j.msec.2017.03.032
0928-4931/

ivory, and changing plaque metabolism by intervening the membrane permeability of bacterium.

Nowadays, several novel treatments are recommended as alternatives to classic methods. Among them, controlled drug delivery systems with minimum side effects are considered superior. These systems are capable of drug release in specific places of the body. Three components of the controlled delivery systems are therapeutic agent, targeting moiety and carrier matrix. The therapeutic agents may be divided as biologicals, like curcumin, and non-biologicals [7–9].

The active component of turmeric is the yellow crystalline compound, curcumin (diferuloylmethane). Over the last century, curcumin has been found to possess antineoplastic, antimicrobial, anti-inflammatory and antioxidant activities. However, it has been rarely used in clinical applications. Poor solubility in aqueous phase, fast degradation and low oral bioavailability are obstacles faced in applying curcumin in therapeutics [10]. In order to load curcumin in NPs, after preparation of NPS, ethanol solution which contained curcumin and Tween 20 was added dropwise under continuous mixing. So, the interaction between NPs and curcumin for curcumin loading happened [11]. One of the possible and profitable ways for curcumin delivery is encapsulation in a nanoparticle platform. Nanoparticles have small size and high surface to volume ratio, which makes them able to pass through biological barriers and ideal for drug delivery [12]. Detection of the loaded curcumin can be accomplished in different ways. One of these methods is electrochemical determination which was studied in NSrGO/Ru@AuNP composites. The results showed successful determination of curcumin in plasma in the range of 0.001–0.1 nM with a detection limit of 2.0×10^{-13} M [13].

Curcumin also has an anti-adhesive effect on oral conditions against *S. mutans* through inhibition of *S. mutans* sortase A, an enzyme responsible for the covalent attachment of Pac proteins to the cell wall in *S. mutans*. This characteristic suggests it as an alternative food-based antimicrobial agent [14,15].

Starch is a polysaccharide that is inexpensive, adaptive and well-known. Since starch is hydrophilic, biocompatible and biodegradable, it is applicable in drug delivery systems. Starch nanoparticles with 10–1000 nm size have been studied as nano-carrier in controlled delivery [16,17]. Alginate is an anionic polysaccharide with negative charge. This material is biocompatible, biodegradable and able to produce gels with polyvalent cations. These polymers are introduced as encapsulating agent and used in drug delivery systems and controlled delivery [18,19]. Chitosan is the *N*-acetylated derivative of chitin, having the structure of β-[1–4]-linked D glucosamine (deacetylated unit) and *N*-acetyl-D-glucosamine. Chitosan is biocompatible with living tissues, hence, it does not cause allergic reactions in the body. It is also biodegradable, whereby it produces non-toxic and easily removable degradation products under fermentation by the colonic bacteria. Since it is soluble in aqueous acidic media, hazardous organic solvents need not to be considered during formulation. As a linear polyamine containing a number of free amine groups, it can be readily cross-linked with various anions. Chitosan has been formulated in controlled release matrixes [20,21].

Chitosan has been used because of exhibiting interactions with surfaces of mucus bearing negative charges and opening the tight junction of Mucous cells. Hydroxyl and primary amine groups in chitosan structure, allows chemical modifications to control physical properties [22,23]. Starch is a type of polysaccharide gaining great attention due to its variety of properties like biodegradability, biocompatibility, low cost and non-toxicity which makes it applicable for nano-drug delivery [24,25]. Alginate is an anionic and water-soluble polysaccharide and can be used widely in drug delivery systems especially for oral route delivery [26].

The objective of the present study was to load the antibacterial polyphenolic drug, curcumin, in biodegradable and biocompatible polysaccharide nanoparticles in order to enhance its bioavailability and to reduce the cariogenic activity of *S. mutans* responsible for dental caries formation. To this end, the preparation process for the synthesis of curcumin-loaded polysaccharide nanoparticles was optimized through response surface methodology of experimental design. Then, the produced nanoparticles and their efficacy against *S. mutans* were assessed by studying the size and morphology of the produced nanoparticles, the drug release profile, determination of minimum inhibitory concentration, and inhibitory effect on *S. mutans* biofilm formation.

2. Materials and methods

S. mutans ATCC 35668 was used as the model cariogenic bacterium throughout the present study. Curcumin, chitosan (low molecular weight), soluble starch, alginate (low viscosity), absolute ethanol and Tween 20 were obtained from Merck (Darmstadt, Germany). Sodium alginate was purchased from Sigma-Aldrich (St. Louis, MO, USA).

For nanoparticle characterization, particle size and polydispersity were assessed using dynamic light scattering (DLS) (NanoBrook Omni, Brookhaven Instruments Co. NY, USA) and SEM (HITACHI S-4160) analyses. DLS was done with a laser light at a wavelength of 657 nm, and a detection angle of 90°. All samples were analyzed for 30 s at 25 °C with five replicates. Nanoparticle surface charge (zeta potential) was measured by means of the same instrument used for DLS. The samples were neutralized (pH of 7.0) before zetametry.

To prepare nanoparticles for SEM analyses, 100 μL of NPs solution was diluted with 3 mL deionized water. Then, it was sonicated for 10–15 min and spread on the surface of glass slides. They were put in silicagel container and dried at 45 °C. Finally, species were covered with Au.

2.1. Nanoparticle preparation

Polysaccharide nanoparticles were produced using the desolvation method by ethanol precipitation of an aqueous polysaccharide solution. The desolvating agent essentially consisted of absolute ethanol with predetermined concentrations of curcumin, as the active substance, and 0.1% Tween 20, as the emulsifying agent.

To prepare curcumin-loaded chitosan nanoparticles, 5 mg/mL chitosan and 0.1% Tween 20 was dissolved in a solution of 1% acetic acid in deionized water. For complete dissolution of chitosan, the solution was stirred for an hour. Next, predetermined amounts of the desolvating agent were added drop-wise under mixing. For making curcumin-loaded alginate nanoparticles, 5 mg/mL alginate and 0.1% Tween 20 was dissolved in deionized water and stirred for 1 h. Then, the desolvating agent was added drop-wise to the alginate solution. In order to prepare curcumin-loaded starch nanoparticles, soluble starch (10 mg/mL) and 0.1% Tween 20 were dissolved in deionized water and the mixture was stirred for an hour at 90 °C ( ).

Then, the desolvating agent was added drop-wise and the solution was stirred for another hour at 70 °C. The resulting nanoparticle suspensions were centrifuged at 10,000 × *g* for 2 min to separate large particles. The supernatant was collected and centrifuged again at 15,000 × *g* for 15 min and the nanoparticle precipitate was washed with 1 mL absolute ethanol to remove free curcumin. Finally, the nanoparticle was re-suspended in deionized water and freeze-dried to produce nanoparticle powders.

2.2. Optimization of loading efficiency of nanoparticles

In the present study, the desolvation method was implemented for curcumin-loaded nanoparticle preparation, and the volume of ethanol (A) and its curcumin concentration (B) were selected as two important factors which affect the loading efficiency. In order to optimize these two factors, response surface method (RSM) was used, and an experiment based on design of experiments (DOE) was performed with the two variants (A, B). According to the design of experiments for two variants, 13 experiments were determined. The range of variant levels in

this statistical optimization method was five levels (Table 2). The curcumin loaded nanoparticles were separated from the reaction medium by centrifugation, the entrapped curcumin was extracted by an ethanolic solution and the UV absorbance of the curcumin was measured at a wavelength of 422 nm. The concentration of curcumin was calculated with reference to a regression equation obtained from a constructed calibration curve of curcumin in absolute ethanol solution.

2.3. Curcumin release from nanoparticles

In vitro curcumin release profiles were assessed according to Kumar Das method (2010) with some modifications. Briefly, lyophilized curcumin-loaded nanoparticles obtained from one set of preparations were re-dispersed in 33 mL of 0.01 M phosphate-buffered saline solution (pH 7.4) at a final concentration of 150 μg/mL. The nanoparticle solution was divided into 33 tubes giving 11 different sets (each set with 3 tubes) for time-dependent release study at time intervals of 0, 2, 4, 6, 12, 24, 36, 48, 60, 72 and 96 h. All sets were incubated at 37 °C under gentle agitation. At predetermined time intervals, curcumin-loaded nanoparticles were first centrifuged at 15,000 ×*g* for 15 min, then the curcumin content was extracted in ethanol under sonication for 15 min and finally quantified spectrophotometrically [27]. The curcumin release was quantified as follows:

$$\text{Release } (\%) = \text{Released curcumin/Free curcumin} \times 100 \quad (1)$$

2.4. Microorganism and culture conditions

S. mutans (ATCC 35668) was used as the model cariogenic microorganism throughout this study. Several colonies from an overnight culture on a blood agar plate were sub-cultured in 15 mL of brain heart infusion broth (BHI) for 24 h at 37 °C, 500 μL of this overnight culture was cultured again in 20 mL of BHI, and the cells were grown until mid-log phase (optical density at 600 nm, 0.5 to 0.6). Then, 15 mL of the mid-log-phase culture was centrifuged at 4000 ×*g* for 18 min at 4 °C and the spent culture medium was discarded [28].

2.5. Determination of MIC for curcumin-loaded nanoparticles against S. mutans

Overnight cultures of *S. mutans* were diluted in BHI to obtain an optical density (OD_{600}) of 0.2 (corresponding to 1×10^8 colony-forming units [CFU]/mL). The inoculum (1 mL for each) was added to vials containing serial dilutions (256 to 0 μL) of a nanoparticle solution with the concentration of 1 mg/mL (experiments performed in triplicate). A control group of bacteria were cultivated in the absence of nanoparticle solution. After incubation for 24 h at 37 °C, bacterial growth was monitored by recording the OD_{600} using a UV–Vis spectrophotometer. The minimum inhibitory concentration (MIC) was defined as the lowest concentration of curcumin-loaded nanoparticles that completely inhibits *S. mutans* growth ($OD_{600} \leq 0.05$) [29].

2.6. The effect of curcumin-loaded nanoparticles on the biofilm formation by S. mutans on dental model

S. mutans was grown (24 h) in a glass vial containing BHI, supplemented with 1% w/v sucrose, at 37 °C. Healthy teeth (without cavities) from healthy individuals were obtained from public clinics and were disinfected and cleaned by immersion in cetrimide, chlorhexidine and ethanol solutions. Then, cylindrical pieces of the teeth enamel (3 mm diameter, 1 mm length) were carved and used for the following experiments. Inoculum, 1 mL, adjusted to 0.1 by BHI at OD_{600}, one piece of disinfected tooth enamel, and curcumin-loaded nanoparticles and pure curcumin were transferred to respective vials and incubated at 37 °C for 24 h. The blank vial contained BHI instead of the inoculum and each test was conducted in three replicates. Then, the culture medium was removed and the enamels were washed three times with sterile physiological serum. In the next step, 1 mL of each nanoparticle solution at its MIC was transferred to a buffer solution (pH 5 or 7), added to the respective vials and incubated for 30 min at 37 °C (both blank and control vials contained 1 mL buffer instead of nanoparticle). Subsequently, the nanoparticle and buffer solutions were removed and the enamels were washed three times with sterile physiological serum in order to remove bacteria in planktonic state. For biofilm fixation, 1 mL ethanol was added to each vial and allowed to rest for 15 min, then, ethanol was extracted and vials were left to air-dry. The biofilms were stained with 1% crystal violet for 10 min. The vials were washed three times with sterile physiological serum to remove unbound crystal violet dye and dried for 2 h at 37 °C. Finally, 1 mL of acetic acid 33% v/v was added to each vial and optical densities were read at 550 nm after 15 min [29,30].

3. Results and discussion

3.1. Preparation and characterization of curcumin-loaded nanoparticles

The loading of curcumin in the polysaccharide nanoparticles increased the solubility of curcumin in the aqueous media. Since the polysaccharide nanoparticles were very hydrophilic in nature with small size and large surface-to-volume ratio, it allows for a greater interaction with the aqueous solvent and thus resulted in the increase of curcumin solubility in the aqueous media.

Particle size distribution of curcumin-loaded chitosan nanoparticles was in the range of 60–85 nm. SEM images confirmed the DLS results and nanoparticles were observed to be spherical in shape with particle sizes within the range of 44–80 nm. The zeta potential was measured to be +21.7 mV. Yadav et al. obtained similar results. They prepared curcumin-loaded chitosan nanoparticles, <50 nm in diameter, cross-linked with glutaraldehyde with the zeta potential of +16.8 mV [20]. The effect of pH during nanoparticle fabrication was investigated. Chuah et al. studied the release of the anticancer agent curcumin from chitosan nanoparticles (CS-NPs). The CS-NPs were ionically gelled with tripolyphosphate (TPP) and registered an isoelectric pH of 6.2 and an average diameter of 214 ± 1.0 nm. Whereas the average diameter of CS-NPs in the present study was almost 66.3 nm. Chuah et al. also evaluated the size and zeta potential of curcumin-loaded CS-NPs in response to variations in titrated pH and found that both the average size and zeta potential were sensitive to the pH of the environment. The zeta potentials of the CS-NPs ranged from +9.15 mV (±1.78 mV) to a maximum of +38.1 mV (±1.02 mV) as the pH was increased from pH 1.2 to pH 3.3 [21]. Similarly, the zeta potential of CS-NPs was analyzed to be +21.7 mV in the present study.

Curcumin-loaded starch nanoparticles were prepared for DLS and zeta potential analysis as suspension with 0.1–0.5 mg/mL and 5 mL volume. Results showed that the size of curcumin-loaded starch nanoparticles was between 50 and 88 nm. Also, zeta potential was reported to be −14.7. In a study conducted by Chin et al., curcumin-loaded starch nanoparticles were synthesized by nanoprecipitation method and water-in-oil micro-emulsion system with almost the same average size of 87 nm [17]. Curcumin-loaded alginate nanoparticles were measured to be 68–116 nm in size. Zeta potential was −23.4 mV. These measurements are shown in Table 1 for all nanoparticles.

Table 1
The size and zeta potential of curcumin-loaded nanoparticles.

Nanoparticle	Size (nm)		Zeta potential (mV)
	Measured with SEM	Measured with DLS	
CNPs	44–66	66.3 ± 1.6	+21.7 ± 1.3
SNPs	50–88	61.1 ± 2.9	−14.7 ± 0.5
ANPs	45–68	78.8 ± 4.2	−23.4 ± 0.5

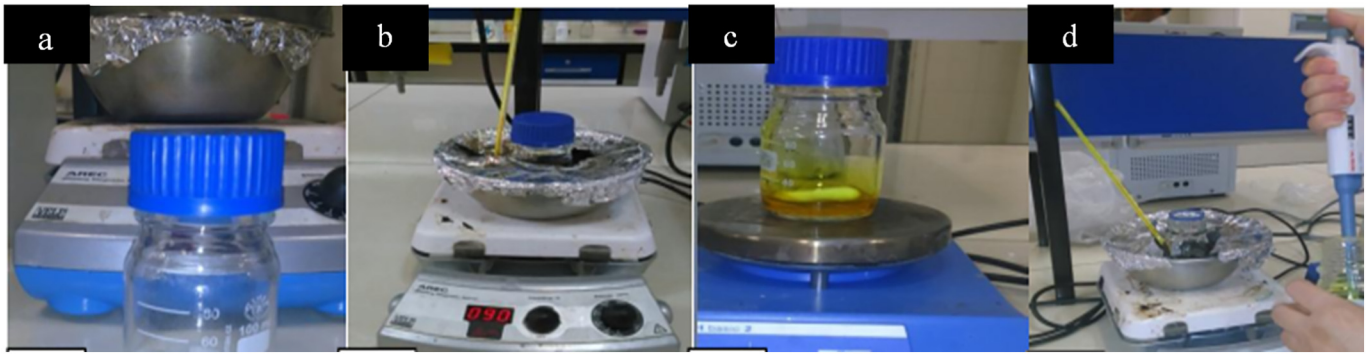

Fig. 1. Starch NP preparation with curcumin loading. a) Starch solution before heating, b) heating of starch solution at 90 °C, c) curcumin solution, d) adding curcumin solution to the starch solution after cooling at 70 °C.

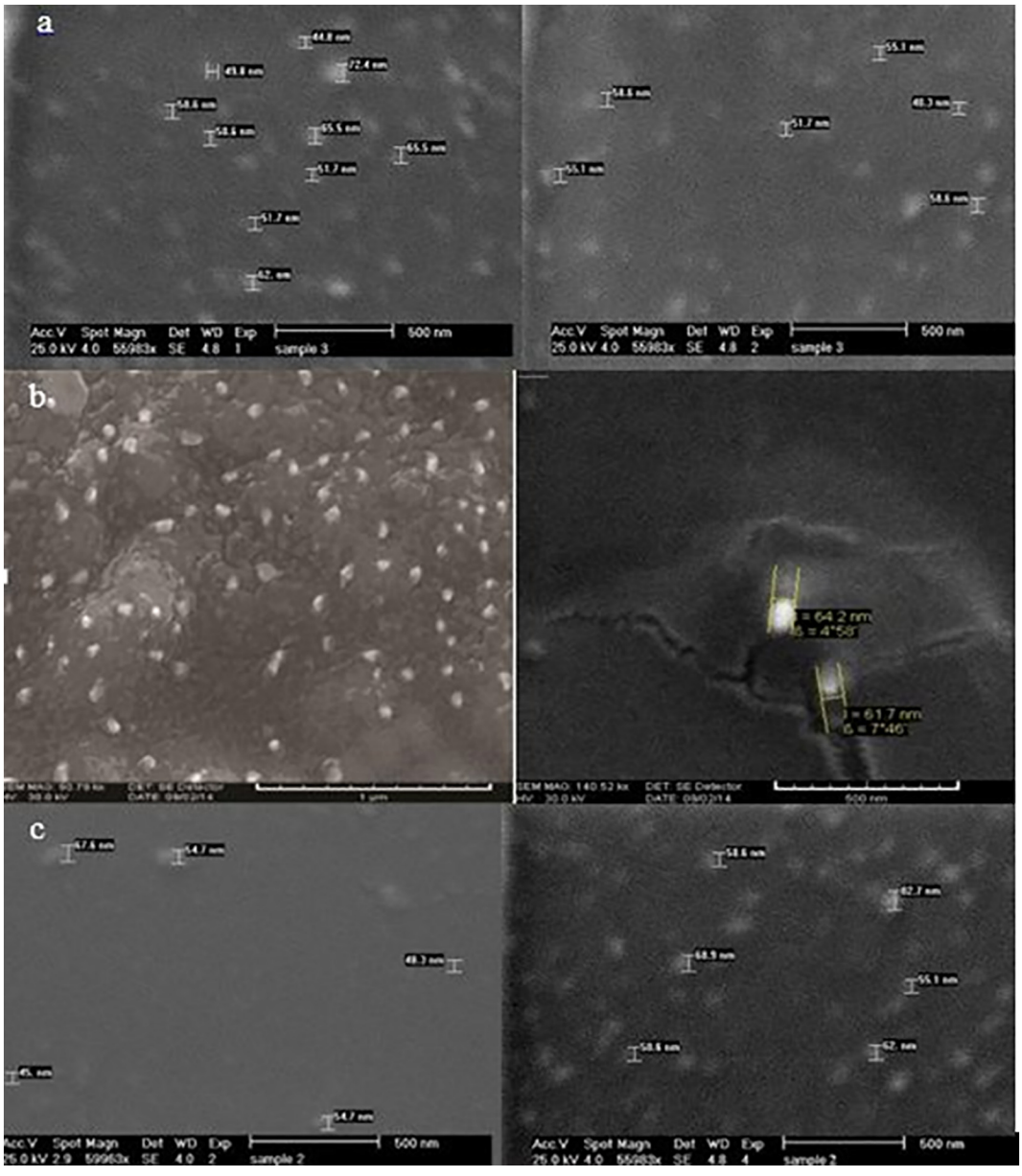

Fig. 2. SEM of curcumin-loaded nanoparticles. a) CNPs, b) SNPs and c) ANPs.

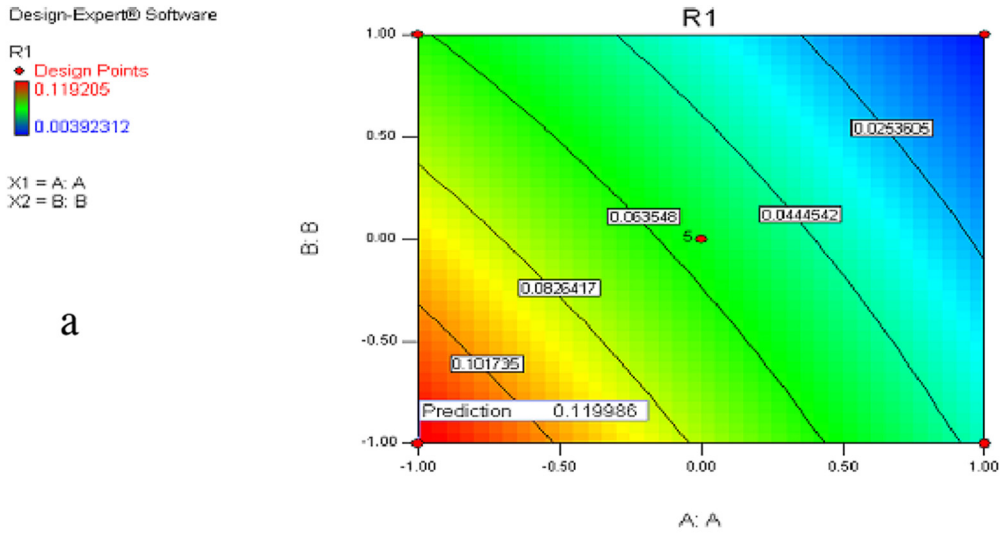

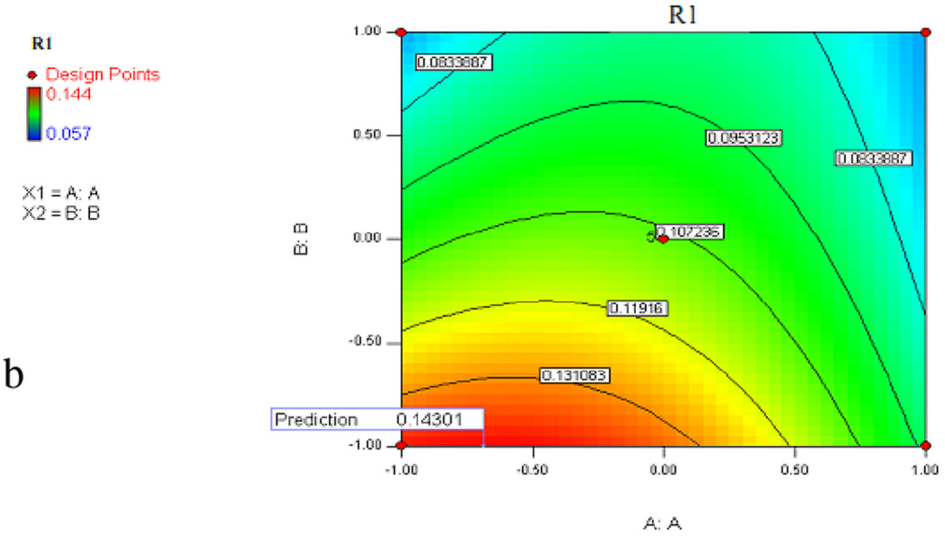

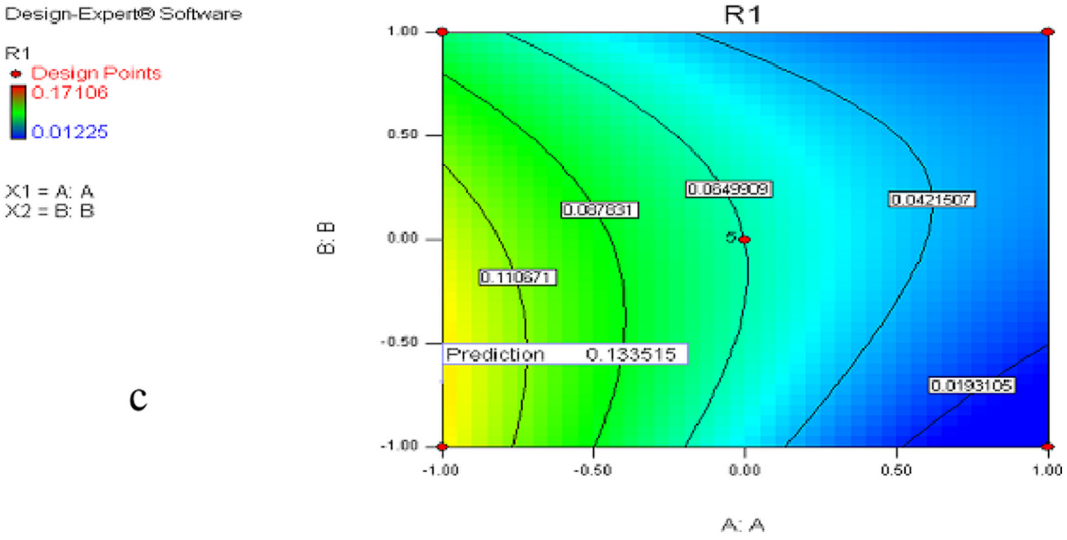

Fig. 3. Two-dimensional illustrations showing the effect of ethanol volume and curcumin concentration on the loading efficiency of polysaccharide nanoparticles. a) Chitosan, b) starch and c) alginate. (For interpretation of the references to color in this figure, the reader is referred to the web version of this article.)

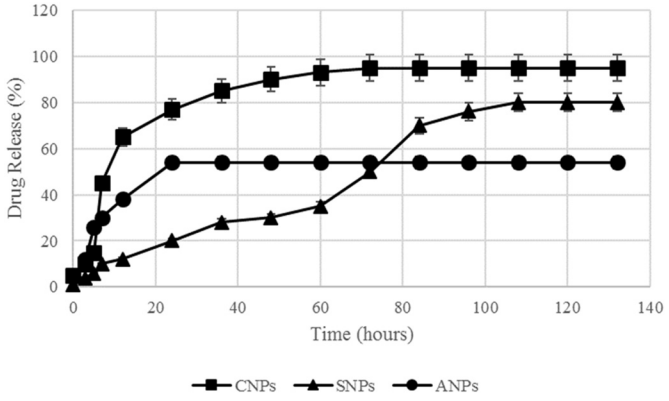

Fig. 4. Release of curcumin from loaded nanoparticles.

Scanning electron microscopy (Fig. 2) showed that alginate and chitosan nanoparticles had uniform dispersion. The sizes acquired from SEM were consistent with the results of DLS analysis. Additionally, Fig. 1 shows that starch NPs were almost spherical with uniform size distribution.

3.2. Optimization of loading efficiency in nanoparticles

Optimization of the curcumin loading efficiency in nanoparticles was performed according to Table 2. The results showed that formulation No. 1 has the highest loading efficiency for chitosan nanoparticles (11.92%). Table 3 presents selected parameters for loading efficiency optimization in curcumin-loaded chitosan nanoparticles. p-Value of <0.05 was considered as safety level of the index efficiency. The p-value for ethanol volume (variant A), curcumin concentration (variant B) and also the interactive effect of ethanol volume and curcumin concentration (AB) are <0.05, so they are significant in the quadratic equation and, therefore, the loading efficiency of curcumin is a function of these terms. Moreover, for the better understanding of the variable model, R-squared is presented. Typically, $R^2 > 0.7$ represents a relatively good correlation coefficient and, when the value of this index is close to 1, experimental data and model of regression will have greater adjustment and, model will have higher accuracy. Therefore, as shown in Table 3 the optimal conditions for loading efficiency of curcumin was obtained with ethanol volume of 1 mL and curcumin concentration of 1.06 mg/mL. Fig. 3.a shows the two-dimensional illustration of parameters effects, ethanol volume and curcumin concentration, on the loading efficiency. According to this figure, for chitosan nanoparticles, with the reduction of ethanol volume (A) and curcumin concentration (B) down to the optimal level (1 mL ethanol and 1.06 mg/mL curcumin), the loading efficiency increases.

Statistical models for the relation of loading efficiency were obtained by RSM for each NP as reported in Table 3. Where R, A and B are loading efficiency, ethanol volume and curcumin concentration, respectively. These models are utilized by the statistical software to predict the optimum conditions, which may happen at levels or level combinations not practically studied in Table 2.

Fig. 3.b shows that by reducing curcumin concentration (B) and ethanol volume (A), loading efficiency of starch nanoparticles increases. In this condition, the optimum condition is 0.143 with $R^2 = 0.97$ for 1.31 mL ethanol volume and 1 mg/mL curcumin concentration. While in Fig. 3.c, red region is not specified, so lower codes related to -1.41 should be noticed in order to get the red region. Also, the optimum condition for alginate nanoparticles is 0.133 with $R^2 = 0.89$.

3.3. Curcumin release from nanoparticles

According to the Fig. 4, chitosan and alginate nanoparticles exhibited a burst release in contrast to starch nanoparticles. At early hours, release rate was high but later, this rate decreased and finally reached to a stationary state. After 12 h, amounts of 63.5% and 36.34% of curcumin were released form chitosan and alginate nanoparticles, respectively, which after 24 h reached 75.3% and 51.2%. Then, the amount of release gradually increased till 96 h for chitosan, 92.8%, and 48 h for alginate nanoparticles, 51.4%. Starch nanoparticles showed a different two-phase release profile, one during 0–60 h and another during 60–132 h. Although starch nanoparticles are hydrophilic, they resist water absorption and swelling till the 60th h, after which they exhibited a second phase of curcumin release. After 12, 24 and 96 h, the amounts of release were 11.1%, 19.3% and 73.4%, respectively.

Chuah et al. investigated the mucoadhesive characteristics and release of the anticancer agent curcumin, entrapped in chitosan nanoparticles (CS-NPs). The CS-NPs were ionically gelled with tripolyphosphate (TPP). Curcumin release from CS-NPs was the least at chitosan to TPP weight ratio of 3:1, with a significant retention (36%) at the end of 6 h

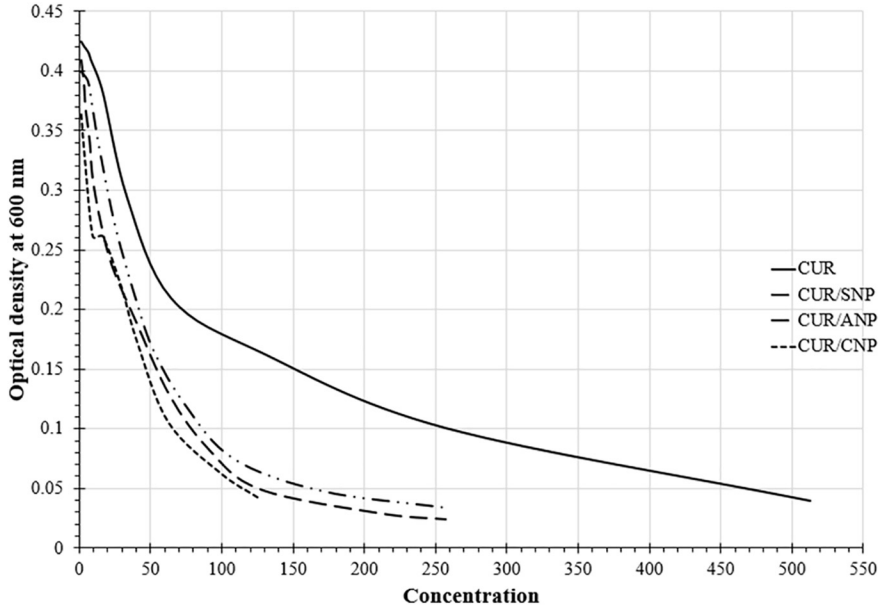

Fig. 5. MIC of pure and loaded curcumin in nanoparticles against *S. mutans*.

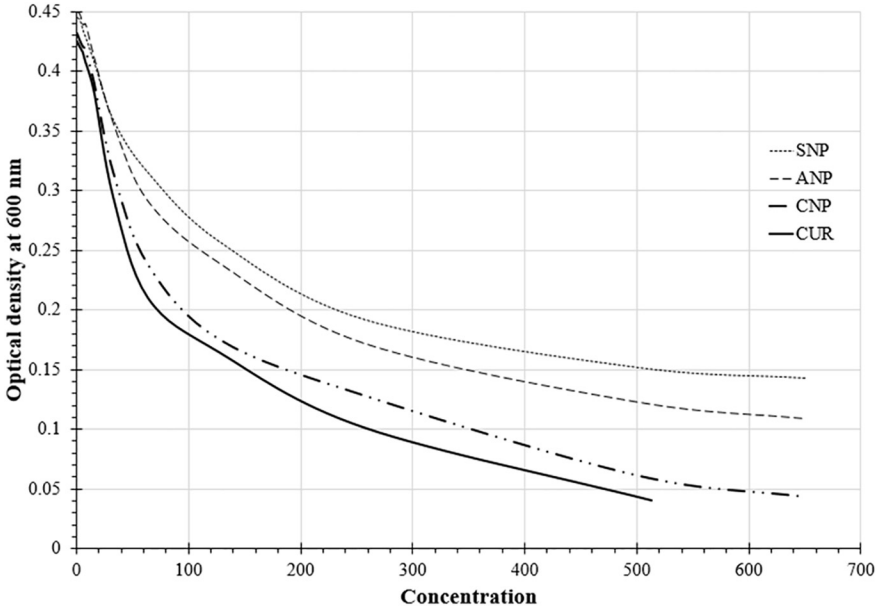

Fig. 6. MIC of pure curcumin and NPs against *S. mutans*.

[21], while in this study curcumin release from CNPs was higher (almost 63.5%) during the initial 12 h. Also, Akhtar et al. investigated oral delivery of curcumin bound to chitosan nanoparticles in order to cure *Plasmodium yoelii* infected mice. They bound curcumin to chitosan nanoparticles to improve its bioavailability and chemical stability. The concentration of curcumin detected in the blood as well as in the red blood cells (RBC) were significantly higher in mice fed with curcumin loaded into chitosan nanoparticles than those administered with equimolar concentration of curcumin only, at all the time points they studied. Oral delivery through chitosan nanoparticles ensured a sustained release of curcumin over 8 h post feeding, whereas, in case of curcumin the levels declined significantly after 3 h and were not detectable beyond 6 h [31].

Chin et al. synthesized curcumin-loaded starch nanoparticles with nano-sintering and water in oil microemulsion methods. About 93% of the entrapped curcumin was gradually released after 240 h [17]. Whereas, in this study release from SNPs reached nearly 80% after 120 h. In another study, starch-based microspheres were prepared and the curcumin release was studied in two media: simulated gastric (SGF, pH 1.2) and intestinal fluids (SIF, pH 6.8). After 96 h, the release reached 95% and 20% in SGF and SIF, respectively. The curcumin release in SIF occurred in two stages. Fast curcumin release in the first stage was related to the adsorbed curcumin at the microsphere surface. High pH of medium leads to curcumin degradation and decrease in the amount of release after 48 h [32].

Raja et al. prepared modified alginate with methyl oleate and used this compound as the curcumin entrapment matrix. Curcumin-release graph showed a stable release pattern for a week after an initial burst release [33]. In the present study, however, 51.4% of the curcumin release form ANPs happened after 48 h. Additionally, Kumar et al. encapsulated curcumin in chitosan-alginate-pluronic composite nanoparticles in order to deliver to cancer cells. Results showed that curcumin released in a controlled way from the composite nanoparticles. After 12 and 24 h the amount of released curcumin was 36% and 51%., respectively, then the amount of release increased gradually to 75% until 96 h [27]. Different compositions of the NPs cause varying amounts of release. Dai et al. studied curcumin release from three various compositions (C3A1, C2A2 and C1A3) of chitosan-alginate (CA) sponge. They showed that after 20 days, about 50% and 70% of curcumin were released from C2A2 and C3A1, respectively. Whereas, the amount of release was 80% from C1A3 after 3 days [34].

Table 2
Different formulations for the optimization of curcumin loading efficiency.

	Ethanol volume (mL)	Curcumin conc. (mg/mL)	Encapsulation efficiency for chitosan (%)	Encapsulation efficiency for starch (%)	Encapsulation efficiency for alginate (%)
1	1	1	11.920	14.3	13.67
2	3	1	4.465	9.6	1.64
3	1	5	6.865	6.7	4.56
4	3	5	1.520	6.7	1.22
5	0.59	3	10.937	9.3	17.11
6	3.41	3	0.393	5.7	2.07
7	2	0.18	9.239	14.4	1.32
8	2	5.82	2.089	9	4.35
9	2	3	5.665	11	6.40
10	2	3	5.164	11.2	5.90
11	2	3	5.245	10.9	6.50
12	2	3	5.333	10.1	6.44
13	2	3	5.176	11.1	6.12

Table 3
Optimal conditions for curcumin loading into nanoparticles.

Codes	Curcumin concentration (mg/mL)	Ethanol volume (mL)	Loading efficiency (R)	Equation
Chitosan	1.06	1	0.119986	$R = 0.058–0.035 \times A - 0.023 \times B + 5.279E-003 \times A \times B$
Starch	1	1.31	0.14301	$R = 0.11 + 0.012 \times A - 0.023 \times B + 0.012 \times A \times B - 0.017 \times A^2$
Alginate	1.62	1	0.133515	$R = 0.065–0.046 \times A - 6.552E-003 \times B + 0.022 \times A \times B + 0.013 \times A^2 - 0.021 \times B^2$

Table 4
MIC of curcumin-loaded and un-loaded NPs.

Free curcumin	Curcumin loaded SNP	Curcumin loaded CNP	Curcumin loaded ANP	Unloaded SNP	Unloaded CNP	Unloaded ANP
0.438	0.204	0.114	0.204	0.781	0.626	0.724

3.4. Inhibitory effect of curcumin-loaded nanoparticles against S. mutans

MIC results of curcumin-loaded nanoparticles and pure curcumin against the pathogenic bacteria in dental caries, S. mutans, are shown in Fig. 5. MIC of curcumin-loaded chitosan, alginate and starch nanoparticles and unloaded NPs can be seen in Table 4.

As shown in Table 4, unloaded NPs have higher MIC and adding curcumin in to them, leads to lower MIC which means anti-bacterial characteristic of curcumin. The results demonstrated that the antimicrobial activity of curcumin was markedly improved by particle size reduction up to the nano range. The reduced size of curcumin in the form of nanoparticles, which is much less than the size of pure curcumin particles, is responsible for more effective penetration and higher uptake by the cells resulting in lower MICs [35]. However, curcumin-loaded chitosan nanoparticles exhibited the best results in terms of MIC. Different mechanisms of interaction with bacteria have been proposed for chitosans. One proposed mechanism is based on the interaction between positively charged chitosan molecules and negatively charged microbial cell membranes leading to the leakage of proteinaceous and other intracellular constituents. Although, at pH 7, free chitosan and the outer chitosan in the nanoparticle complexes are expected to be neutral, but chitosan within the particle may retain its charge. A second proposed mechanism is based on binding of chitosan with microbial DNA, in turn interfering with mRNA and protein synthesis, which clearly requires entry of the chitosan into the cell [3].

The comparison between Fig. 5 and Fig. 6 shows that the amount of reduction in optical density of NPs isn't <0.05 that means the anti-bacterial property.

3.5. Inhibitory effect of curcumin-loaded nanoparticles on S. mutans biofilm formation at different pHs

Sortase A is an enzyme responsible for the covalent attachment of Pac proteins to the cell wall in *S. mutans*. It has been shown to play a role in modulating the surface properties and the biofilm formation and influence the cariogenicity of *S. mutans* [15,36,37]. Curcumin has been reported to inhibit sortase A activity in *Staphylococcus aureus in vitro* [36]. Although the conserved cysteine 184 and histidine 120 residues, which are essential for *S. aureus* sortase A activity, are found in *S. mutans* UA159 sortase A [37], curcumin can inhibit purified *S. mutans* sortase A with a half-maximal inhibitory concentration (IC50) of (10.2 ± 0.7) μmol/L, which is lower than minimum inhibitory concentration (MIC) of 175 μmol/L. Curcumin (15 μmol/L) was found to release the Pac protein to the supernatant and reduce *S. mutans* biofilm formation [15].

S. mutans is well-known for its ability to form biofilms in the oral niche [38]. Thus, the ability of the curcumin-loaded nanoparticles to block biofilm formation was examined. Tooth sections were inoculated with *S. mutans* and incubated with curcumin-loaded nanoparticles and pure curcumin. According to the obtained results (Table 5), it was found that the inhibitory effect of the curcumin loaded in nanoparticles was higher than similar amount of pure curcumin in both pH 5 and 7. The possible explanation is that the reduced size of nanoparticles leads to enhanced diffusion and higher adsorption by cells. Accordingly, peptidoglycan membrane will be disrupted and bacterium will die easier.

Also, the inhibitory effect of chitosan and alginate nanoparticles at pH 5 was higher than pH 7. In the case of chitosan, this influence may be due to free amino groups being neutral at pH 7 compared with pH 5, which causes more interactions between positively charged chitosan molecules and negatively charged microbial cell membranes.

Curcumin has low water insolubility (<1 μg/mL) and the release of it has created many challenges. The results showed that in acid environment, by covalently conjugating curcumin on the hydrophilic terminals of pluronic F68 chains *via* cis-aconitic anhydride linkers, curcumin release rapidly. After 96 h, almost 60% of curcumin was released at pH 5, while only 40% of curcumin was released at pH 7.4 [39]. Additionally, a study about formation of Formation of Curcumin-Eudragit® EPO Molecular Complexes (CEMCs) was conducted to improve water solubility. Water solubility of CEMCs was higher in acidic pH rather than neutral pH [40].

4. Conclusions

Antibiotic resistance has prompted the search for new agents that can inhibit bacterial growth. The antibiofilm activities of nanosized curcumin-loaded particles synthesized by desolvation method are reported. In the present work, nanoparticulate systems were investigated for their characteristics against *S. mutans* function on dental model. Curcumin was utilized as a biological antibacterial agent for loading into nanoparticles. Results showed that the size of produced nanoparticles with starch, chitosan and alginate were 61.1, 66.3 and 78.8 nm, respectively. Also, the zeta potential was −14.7, +21.7 and −23.4 mV, respectively. The maximum amount of curcumin load in nanoparticles was for chitosan (51.03), which for starch and alginate were 24.59 and 29.69, respectively. The MIC was found for chitosan nanoparticles to be 0.114 mg/mL, when alginate and starch nanoparticles showed an MIC of 0.204 mg/mL. Additionally, nanoparticles have more inhibitory effects comparing with the free curcumin. Chitosan nanoparticles exhibited the best inhibitory effect in comparison with other nanoparticle types especially in lower pH. In the release analysis, chitosan and alginate showed burst release that for chitosan after 96 h and for alginate after 48 h, the amount of release were 92.8% and 51.4%, respectively. Whereas, starch nanoparticles showed a more stable release. After reaching to equilibrium point at the end of 122 h, 81.6% of curcumin was released. The effect of curcumin-loaded nanoparticles on *S. mutans* biofilms was also assessed on dental models. Based on the acquired results, curcumin-loaded chitosan nanoparticles hold promises for being used in dental decay fighting products.

Table 5
Optical densities and percentage decreases obtained from biofilms after exposure to curcumin loaded nanoparticles and pure curcumin in pH 5 and 7.

Test	Blank (OD_{550})	Pure curcumin (%)	Unloaded CNPs (%)	Unloaded SNPs (%)	Unloaded ANPs (%)	Curcumin loaded CNPs (%)	Curcumin loaded SNPs (%)	Curcumin loaded ANPs (%)
pH 5	0.932	67.38	26.17	21.82	26.26	95.49	89.48	95.28
pH 7	0.772	59.97	26.04	28.39	26.56	93.78	99.38	93.13

Acknowledgement

Hereby, the authors acknowledge the financial support from the Iranian National Science Foundation (grant number 92020975).

References

[1] S. Nguyen, M. Hiorth, M. Rykke, G. Smistad, The potential of liposomes as dental drug delivery systems, Eur. J. Pharm. Biopharm. 77 (2011) 75–83.
[2] O.A. Hamed, N. Mehdawi, A. Abu Taha, E.M. Hamed, M.A. Al-Nuri, A.S. Hussein, Synthesis and antibacterial activity of novel curcumin derivatives containing heterocyclic moiety, Iranian Journal of Pharmaceutical Research: IJPR 12 (2013) 47–56.
[3] L.E. Chavez de Paz, A. Resin, K.A. Howard, D.S. Sutherland, P.L. Wejse, Antimicrobial effect of chitosan nanoparticles on streptococcus mutans biofilms, Appl. Environ. Microbiol. 77 (2011) 3892–3895.
[4] B. Nagavarma, H.K. Yadav, A. Ayaz, L. Vasudha, H. Shivakumar, Different techniques for preparation of polymeric nanoparticles—a review, Asian J. Pharm. Clin. Res 5 (2012) 16–23.
[5] S. Biswas, I. Biswas, Role of HtrA in surface protein expression and biofilm formation by *Streptococcus mutans*, Infect. Immun. 73 (2005) 6923–6934.
[6] M. Hannig, C. Hannig, Nanomaterials in preventive dentistry, Nat. Nanotechnol. 5 (2010) 565–569.
[7] J.A. Cury, L.M. Tenuta, Enamel remineralization: controlling the caries disease or treating early caries lesions? Brazilian Oral Research 23 (Suppl. 1) (2009) 23–30.
[8] D.K. Shvero, M.P. Davidi, E.I. Weiss, N. Srerer, N. Beyth, Antibacterial effect of polyethyleneimine nanoparticles incorporated in provisional cements against *Streptococcus mutans*, J. Biomed. Mater. Res. B Appl. Biomater. 94 (2010) 367–371.
[9] K. Park, Controlled drug delivery systems: Past forward and future back, J. Control. Release 190 (2014) 3–8.
[10] A.E. Krausz, B.L. Adler, V. Cabral, M. Navati, J. Doerner, R.A. Charafeddine, D. Chandra, H. Liang, L. Gunther, A. Clendaniel, Curcumin-encapsulated nanoparticles as innovative antimicrobial and wound healing agent, Nanomedicine: Nanotechnology, Biology and Medicine 11 (2015) 195–206.
[11] W. Fan, W. Yan, Z. Xu, H. Ni, Formation mechanism of monodisperse, low molecular weight chitosan nanoparticles by ionic gelation technique, Colloids Surf. B: Biointerfaces 90 (2012) 21–27.
[12] G. Flora, D. Gupta, A. Tiwari, Nanocurcumin: A Promising Therapeutic Advancement over Native Curcumin, Critical Reviews™ in Therapeutic Drug Carrier Systems, 2013 30.
[13] G. Kotan, F. Kardas, O.A. Yokus, O. Akyldrm, H. Saral, T. Eren, M.L. Yola, N. Atar, A novel determination of curcumin via Ru@Au nanoparticle decorated nitrogen and sulfur-functionalized reduced graphene oxide nanomaterials, Anal. Methods 8 (2016) 401–408.
[14] J. Song, B. Choi, E.-J. Jin, Y. Yoon, K.-H. Choi, Curcumin suppresses *Streptococcus mutans* adherence to human tooth surfaces and extracellular matrix proteins, Eur. J. Clin. Microbiol. Infect. Dis. 31 (2012) 1347–1352.
[15] P. Hu, P. Huang, M.W. Chen, Curcumin reduces *Streptococcus mutans* biofilm formation by inhibiting sortase A activity, Arch. Oral Biol. 58 (2013) 1343–1348.
[16] M. Sun, X. Su, B. Ding, X. He, X. Liu, A. Yu, H. Lou, G. Zhai, Advances in nanotechnology-based delivery systems for curcumin, Nanomedicine (London, England) 7 (2012) 1085–1100.
[17] S.F. Chin, S.N.A. Mohd Yazid, S.C. Pang, Preparation and characterization of starch nanoparticles for controlled release of curcumin, International Journal of Polymer Science 2014 (2014).
[18] H. Daemi, M. Barikani, Synthesis and characterization of calcium alginate nanoparticles, sodium homopolymannuronate salt and its calcium nanoparticles, Scientia Iranica 19 (2012) 2023–2028.
[19] S.K. Nitta, K. Numata, Biopolymer-Based Nanoparticles for Drug/Gene Delivery and Tissue Engineering, Int. J. Mol. Sci. 14 (2013) 1629–1654.
[20] A. Yadav, V. Lomash, M. Samim, S.J. Flora, Curcumin encapsulated in chitosan nanoparticles: a novel strategy for the treatment of arsenic toxicity, Chem. Biol. Interact. 199 (2012) 49–61.
[21] L.H. Chuah, N. Billa, C.J. Roberts, J.C. Burley, S. Manickam, Curcumin-containing chitosan nanoparticles as a potential mucoadhesive delivery system to the colon, Pharm. Dev. Technol. 18 (2013) 591–599.
[22] A. Kumari, S.K. Yadav, S.C. Yadav, Biodegradable polymeric nanoparticles based drug delivery systems, Colloids Surf. B: Biointerfaces 75 (2010) 1–18.
[23] L. Mazzarino, C. Travelet, S. Ortega-Murillo, I. Otsuka, I. Pignot-Paintrand, E. Lemos-Senna, R. Borsali, Elaboration of chitosan-coated nanoparticles loaded with curcumin for mucoadhesive applications, J. Colloid Interface Sci. 370 (2012) 58–66.
[24] M.R. Mauricio, P.G. da Costa, S.K. Haraguchi, M.R. Guilherme, E.C. Muniz, A.F. Rubira, Synthesis of a microhydrogel composite from cellulose nanowhiskers and starch for drug delivery, Carbohydr. Polym. 115 (2015) 715–722.
[25] D. Narayanan, S. Nair, D. Menon, A systematic evaluation of hydroxyethyl starch as a potential nanocarrier for parenteral drug delivery, Int. J. Biol. Macromol. 74 (2015) 575–584.
[26] G. Garrait, E. Beyssac, M. Subirade, Development of a novel drug delivery system: chitosan nanoparticles entrapped in alginate microparticles, J. Microencapsul. 31 (2014) 363–372.
[27] R.K. Das, N. Kasoju, U. Bora, Encapsulation of curcumin in alginate-chitosan-pluronic composite nanoparticles for delivery to cancer cells, Nanomedicine: Nanotechnology, Biology and Medicine 6 (2010) 153–160.
[28] J. Jefferies, L. Nieminen, L.-A. Kirkham, C. Johnston, A. Smith, T.J. Mitchell, Identification of a secreted cholesterol-dependent cytolysin (mitilysin) from *Streptococcus mitis*, J. Bacteriol. 189 (2007) 627–632.
[29] T.B.L. Bedran, L. Grignon, D.P. Spolidorio, D. Grenier, Subinhibitory concentrations of triclosan promote *Streptococcus mutans* biofilm formation and adherence to oral epithelial cells, PLoS One 9 (2014), e89059. .
[30] S. Stepanović, D. Vuković, I. Dakić, B. Savić, M. Švabić-Vlahović, A modified microtiter-plate test for quantification of staphylococcal biofilm formation, J. Microbiol. Methods 40 (2000) 175–179.
[31] F. Akhtar, M.M.A. Rizvi, S.K. Kar, Oral delivery of curcumin bound to chitosan nanoparticles cured *Plasmodium yoelii* infected mice, Biotechnol. Adv. 30 (2012) 310–320.
[32] A.G.B. Pereira, A.R. Fajardo, S. Nocchi, C.V. Nakamura, A.F. Rubira, E.C. Muniz, Starch-based microspheres for sustained-release of curcumin: preparation and cytotoxic effect on tumor cells, Carbohydr. Polym. 98 (2013) 711–720.
[33] M. Ali Raja, C. Liu, Z. Huang, Nanoparticles based on oleate alginate ester as curcumin delivery system, Current Drug Delivery 12 (2015) 613–627.
[34] M. Dai, X. Zheng, X. Xu, X. Kong, X. Li, G. Guo, F. Luo, X. Zhao, Y.Q. Wei, Z. Qian, Chitosan-alginate sponge: preparation and application in curcumin delivery for dermal wound healing in rat, Biomed. Res. Int. 2009 (2009).
[35] R.K. Basniwal, H.S. Buttar, V. Jain, N. Jain, Curcumin nanoparticles: preparation, characterization, and antimicrobial study, J. Agric. Food Chem. 59 (2011) 2056–2061.
[36] B.-S. Park, J.-G. Kim, M.-R. Kim, S.-E. Lee, G.R. Takeoka, K.-B. Oh, J.-H. Kim, *Curcuma longa* L. constituents inhibit sortase A and *Staphylococcus aureus* cell adhesion to fibronectin, J. Agric. Food Chem. 53 (2005) 9005–9009.
[37] A.M. Perry, H. Ton-That, S.K. Mazmanian, O. Schneewind, Anchoring of surface proteins to the cell wall of *Staphylococcus aureus*. III. Lipid II is an in vivo peptidoglycan substrate for sortase-catalyzed surface protein anchoring, J. Biol. Chem. 277 (2002) 16241–16248.
[38] Z.T. Wen, R.A. Burne, Functional genomics approach to identifying genes required for biofilm development by *Streptococcus mutans*, Appl. Environ. Microbiol. 68 (2002) 1196–1203.
[39] X.-B. Fang, J.-M. Zhang, X. Xie, D. Liu, C.-W. He, J.-B. Wan, M.-W. Chen, pH-sensitive micelles based on acid-labile pluronic F68-curcumin conjugates for improved tumor intracellular drug delivery, Int. J. Pharm. 502 (2016) 28–37.
[40] S. Kumar, S.S. Kesharwani, H. Mathur, M. Tyagi, G.J. Bhat, H. Tummala, Molecular complexation of curcumin with pH sensitive cationic copolymer enhances the aqueous solubility, stability and bioavailability of curcumin, Eur. J. Pharm. Sci. 82 (2016) 86–96.